Cabin Noise Reduction: An Integrated Approach for Agricultural Tractors

Marco Polastri[a] | Stefano Mischiari[a] | Paolo Bonfiglio[b]*

[a] Carraro Group,
Via Olmo, 3, 35011 Campodarsego (PD)
[b] Materiacustica Srl,
Via Ravera, 15A, 44122 Ferrara
* Corresponding author:
paolo.bonfiglio@materiacustica.it

Ricevuto: 2/12/2025
Accettato: 4/2/2026

DOI: 10.3280/riaof-2026oa21543
ISSNe: 2385-2615

This paper examines noise and vibration phenomena inside the cabin of an agricultural tractor under various operating conditions. The experimental setup, including tractor specifications and measurement configuration, is described in detail. A preliminary analysis characterizes noise and vibration levels at selected cabin positions and explores correlations between sources, propagation paths, and perceived acoustic discomfort. Further experiments quantify the contribution of individual sources to overall noise. Based on these findings, the most effective noise-reduction strategies are implemented and their impact evaluated.
Keywords: agricultural tractor cabin acoustics, source contribution quantification, propagation paths, acoustic discomfort

Riduzione del rumore in cabina: un approccio integrato per i trattori agricoli
Questo articolo analizza i fenomeni di rumore e vibrazione all'interno della cabina di un trattore agricolo in diverse condizioni operative. Il set-up sperimentale, comprensivo delle specifiche del trattore e della configurazione di misura, è descritto in dettaglio. Viene condotta un'analisi preliminare per caratterizzare i livelli di rumore e vibrazione in posizioni selezionate della cabina e per identificare le correlazioni tra sorgenti, percorsi di propagazione e discomfort acustico percepito. Ulteriori indagini sperimentali quantificano il contributo delle singole sorgenti al livello sonoro complessivo. Sulla base di tali risultati, vengono implementate le strategie di riduzione del rumore più efficaci e ne viene valutato l'impatto.
Parole chiave: acustica della cabina di trattore agricolo, contributo delle sorgenti, percorsi di propagazione, comfort acustico

1 | Introduction

Reducing noise levels inside agricultural tractor cabins is essential to safeguard operator health, safety, comfort, and productivity. Prolonged exposure to excessive noise levels can lead to noise-induced hearing loss and cardiovascular disorders such as hypertension [1] [2]. European regulations impose strict limits on workplace noise exposure. Directive 2003/10/EC establishes a daily exposure limit of 87 dBA, considering the attenuation provided by personal protective equipment, and sets lower and upper action values at 80 dBA and 85 dBA, respectively [3]. Furthermore, Regulation (EU) 1322/2014 [4], applicable under Regulation (EU) 167/2013 [5], specifies technical requirements for vehicle approval, including acoustic protection for occupants.

From an operational safety perspective, an acoustically disturbed environment can impair concentration and alertness, increasing the risk of errors and accidents. Reduced perception of external auditory signals, such as alarms or warning calls, may result in severe consequences in complex agricultural contexts [2]. Regarding comfort and productivity, a quieter cabin enhances operator well-being, reduces fatigue, and promotes efficiency during extended work periods. Studies in industrial settings indicate that noise can cause irritability, sleep disturbances, and decreased performance [6]. Although specific studies on the commercial impact of low-noise tractors are lacking, acoustic comfort is widely regarded as a competitive factor influencing purchasing decisions and shaping perceptions of equipment quality and innovation.

Numerous studies have investigated vibro-acoustic phenomena in agricultural tractors, aiming to reduce noise and vibration for improved operator comfort. Early research [7] proposed vibro-acoustic optimization of tractor cabins through combined experimental and numerical approaches, emphasizing the role of structural modifications in noise mitigation. Understanding tire-soil interaction is critical; in [8], a multibody approach based on the lumped parameter method was introduced to evaluate tractor dynamics and determine loads transmitted to the cabin under realistic operating conditions. Advanced NVH (Noise, Vibration, and Harshness) system simulations validated by experimental measurements have been developed [9], while active noise control (ANC) has been explored under controlled workloads and field tests using adaptive algorithms [10]. Optimization of cabin mounting systems through genetic algorithms has been proposed to minimize vibration levels [11], and experimental validation of theoretical noise fields around trac-

tors has highlighted the importance of propagation paths [12]. Further contributions [13] [14] enriched this domain by performing experimental analyses of noise and vibration under normal and predefined working conditions, focusing on acoustic comfort and psychoacoustic parameters such as loudness, sharpness, and roughness. These studies also assessed the effectiveness of various vibration control systems (including suspension configurations, seat designs, and tire technologies) through comparative tests on multiple tractor models. Collectively, these investigations provide a comprehensive framework for understanding noise and vibration sources, propagation mechanisms, and mitigation strategies in agricultural tractors.

The structure of this paper is as follows: Section 2 describes the tractor used in the experimental study, the measurement setup, and the operational conditions adopted. Section 3 presents the preliminary analysis aimed at characterizing noise and vibration levels at specific cabin positions and identifying correlations between sources, propagation paths, and perceived noise. Subsequent sections illustrate further experimental investigations conducted to quantify the contribution of each source. The results obtained after implementing the most effective noise-reduction interventions are then discussed. Finally, the concluding section outlines key findings and future research directions.

2 | Materials and methods

2.1 | Description of the tractor

The vehicle is a 2025 utility tractor equipped with a 3.6-liter, four-cylinder engine delivering a rated power of up to 85 kW. The brand and model of the tractor are not disclosed in the article for confidentiality reasons. It features a CARRARO T135 transaxle transmission with two powershift speeds, three mechanically controlled ranges, and six mechanical gears. Additional components include 4WD, three-speed rear power take-offs, and a single-speed front PTO. The hydraulic system comprises three gear pumps: one dedicated to the hydraulic steering unit (HSU), power braking, oil cooling, and transmission functions, and two pumps serving the rear hitch and external hydraulic consumers. An air compressor for trailer braking is also integrated.

The operator workspace consists of a six-pillar cabin mounted to the driveline via four anti-vibration mounts (Type CB 80 silent blocks [15]). Each mount comprises two natural rubber discs with a diameter of 76 mm and an overall height of 95 mm when assembled in pairs. These mounts are available in different Shore hardness values and can withstand a maximum axial load of 200 kg. Given that the load on each cab support is approximately 170 kg, CB 80 mounts with a hardness of 65 Shore were selected as the only configuration compatible with the current housing geometry.

2.2 | Description of the measurement set-up

The experimental measurement setup was conducted using the following instrumentation:

- PCB 378B02 microphones (nominal sensitivity 50 mV/Pa) positioned near the operator's ears;
- PCB 356B21 accelerometers (nominal sensitivity 10 mV/g) positioned on the hydraulic steering unit (hereafter HSU) and on the handbrake tie rod (hereafter Handbrake);
- PCB 353B18 accelerometers (nominal sensitivity 10 mV/g) positioned on the front firewall, on the brake pipe attached to the firewall and on the brake pump;
- Kistler 8766A500BH accelerometers (nominal sensitivity 1000 mV/g) located upstream and downstream of the front (left side) and rear (right side) silent blocks.

Data acquisition was carried out using Siemens Simcenter Testlab 2406 system. The microphone, accelerometric, and pressure signals were recorded at a sampling frequency of 25600 Hz, while the engine speed signal was captured at a sampling frequency of 200 Hz using a tachometric sensor on the crankshaft and a dedicated CAN bus transfer protocol.

2.3 | Description of testing conditions

The experimental campaign carried out at Prototypes and validation department of CARRARO Agritalia included the following types of tests:

- **static measurements** (tractor at rest) at fixed engine speed values of 850 rpm, 1000 rpm, 1200 rpm, 1650 rpm, 1950 rpm, 2100 rpm, and 2450 rpm;
- **static measurements** (tractor at rest) varying the engine speed continuously from 850 rpm to 2450 rpm;
- **dynamic measurements** under conditions of the vehicle operating at 2450 rpm and a speed of 8 km/h.

For each experimental trial, sound pressure and acceleration signals were processed to calculate the overall levels (expressed in dBA) at the microphones, third-octave band spectra, narrowband spectra with a resolution of 1 Hz, and time histories of the overall microphone and acceleration levels. Each test was repeated three times, and for each measured quantity, the average energy values were determined. To summarize the results related to noise levels, the maximum value (both in the time domain and the frequency domain) between the two microphones will be reported, ensuring that the most demanding condition for the operator is always considered.

3 | Results

3.1 | Preliminary survey

Fig. 1 presents the spectrogram of the envelope from the microphones during a static measurement, where the engine speed was continuously varied from 850 rpm to 2450 rpm. The frequency range analysed extends up to 2000 Hz.

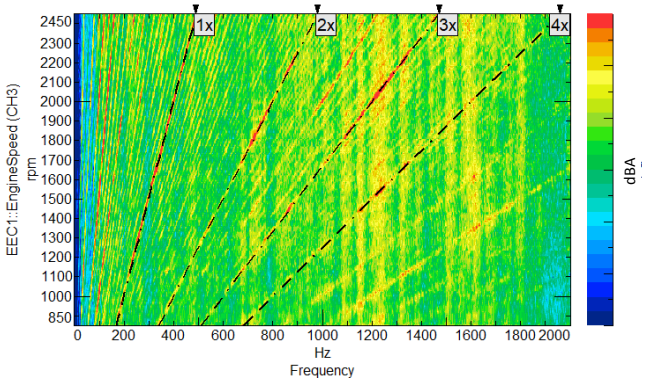

Fig. 1 – Spectrogram of the microphone envelope related to a static measurement varying the rotational speed from 850 rpm to 2450 rpm

Spettrogramma dell'inviluppo dei microfoni relativo ad una misura statica variando in rampa continua il numero di giri da 850 rpm a 2450 rpm

This spectrogram provides insights into the frequency distribution and amplitude changes of the sound over the specified range, facilitating a deeper understanding of the acoustic behaviour of the tractor during different engine speeds.

The graph clearly highlights spectral components at frequencies below 200 Hz, attributed to combustion orders. More notably, a dominant component is observed at frequencies of 170 Hz at 850 rpm and 490 Hz at 2450 rpm. This component can be linked to the operation of pumps, characterized by 12 teeth.

Additionally, a significant presence of spectral content above 1000 Hz is detected, negatively affecting the perceived sound quality, rendering it unsatisfactory.

An alternative representation of microphones response is shown in Fig. 2, which displays the narrowband spectra for all analysed engine speed values during the static tests. The comparison among different operating conditions clearly reveals components related to the combustion process, hydraulic components, and those localized at frequencies above 1000 Hz.

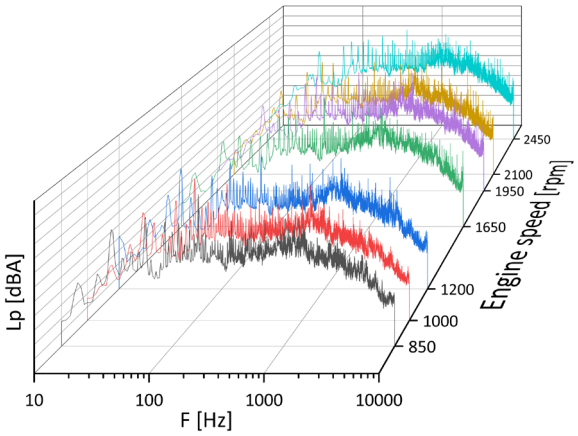

Fig. 2 – Narrowband sound spectra of the microphone envelope for static measurements at fixed engine speeds

Spettri sonori in banda fine dell'inviluppo dei microfoni per le misure statiche a numero fisso di giri motore

To illustrate the distinctive characteristics of the noise perceived within the cabin, figures 3 and 4 present the third-octave band spectra acquired from the microphones under static conditions at 850 rpm and 2450 rpm.

Additionally, these figures include the spectra from the accelerometers installed at various significant points: on the firewall, HSU, handbrake, brake pipe, brake pump, and in two positions inside the cabin, near the silent blocks.

This comparative analysis allows for a comprehensive understanding of how different sources contribute to the overall noise profile within the cabin at varying engine speeds.

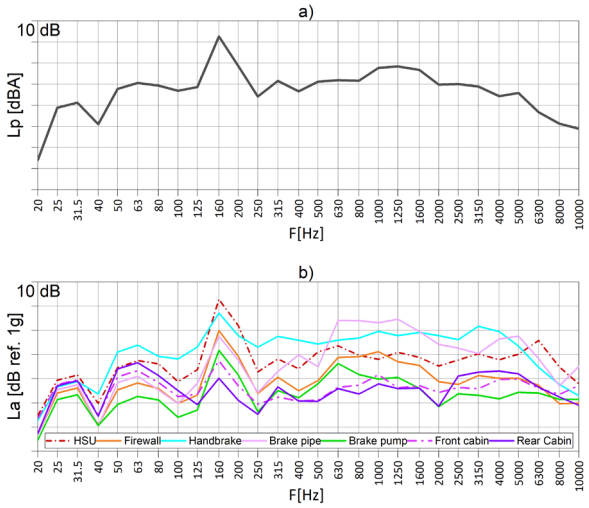

Fig. 3 – Frequency spectra of a) the microphone envelope and b) the accelerometers for the static measurement at 850 rpm

Spettri in frequenza a) dell'inviluppo dei microfoni e b) degli accelerometri per la misura statica a 850 rpm

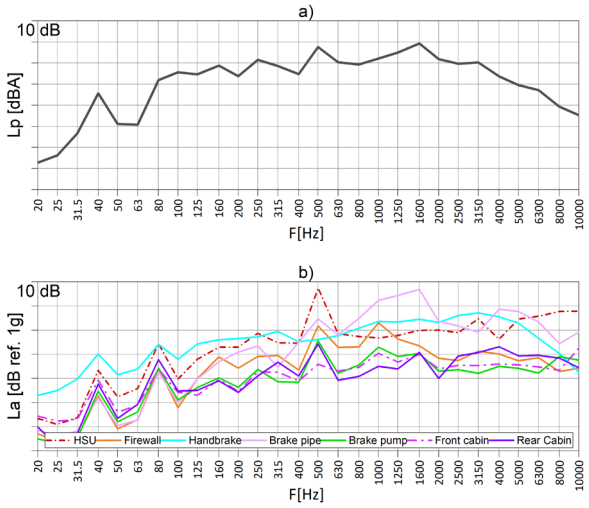

Fig. 4 – Frequency spectra of a) the microphone envelope and b) the accelerometers for the static measurement at 2450 rpm

Spettri in frequenza a) dell'inviluppo dei microfoni e b) degli accelerometri per la misura statica a 2450 rpm

The preceding figures not only clearly highlight the characteristics of the previously described noise but also allow for the correlation of acoustic components to the accelerations measured at various points within the cabin.

In particular:

- **Hydraulic Components**: frequency components located in the band of 160 Hz at 850 rpm and 500 Hz at 2450 rpm are significantly present near the HSU, as expected. These components also exhibit considerable amplitudes on the firewall (justified by the rigid connection between the firewall and the HSU) and on the brake pipe. At 850 rpm, notable stresses are observed on the handbrake. To a lesser extent, the same components are detectable at the base of the cabin, near the silent blocks.
- **High-Frequency Noise**: the noise at frequencies above 1000 Hz is primarily associated with the vibration of the brake pipe but is also manifested, albeit at a lower intensity, on the firewall, HSU, and handbrake.

The pairs of accelerometers positioned upstream and downstream of the silent blocks were used to calculate the transmissibility of these supports. Transmissibility is computed as the ratio between the upstream and downstream acceleration signals; therefore, high transmissibility function values indicate high vibration-isolation performance.

To evaluate the vibration isolation capabilities of the anti-vibration mounts, dynamic measurements were conducted by bringing the tractor to a constant speed of 40 km/h and then shutting off the engine until the vehicle came to a complete stop. This procedure allowed for the exclusion of contributions from alternative propagation paths (particularly those associated with the HSU and the pipes connected to the cabin) from the signals acquired by the accelerometers positioned downstream of the supports. The transmissibility curves for the front and rear supports are presented in Fig. 5.

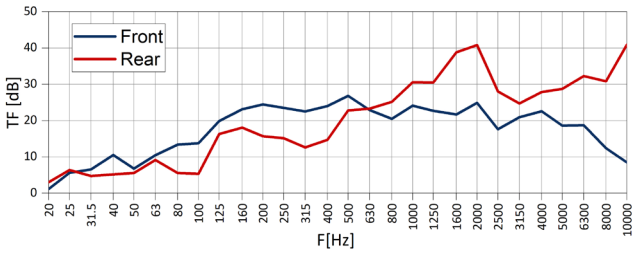

Fig. 5 – Transmissibility functions (in 1/3 octave bands) for front and rear silent blocks

Funzioni di trasmissibilità (in 1/3 di ottava) per i supporti antivibranti anteriori e posteriori

The analysis of the transmissibility function has revealed suboptimal behaviour of the silent blocks. Specifically, the front support exhibits an increasing filtering capacity up to approximately 500 Hz, although with a modest slope. Beyond this frequency, the transmissibility tends to stabilize, reaching a plateau condition. In contrast, the rear support generally demonstrates limited isolating capacity, except in the frequency bands centered around 1600 Hz and 2000 Hz, where significantly better performance is observed.

These preliminary results highlight the need for a deeper analysis of the dynamic characteristics of the silent blocks, additional propagation paths (particularly those associated with the pipes and the handbrake), as well as the pumps responsible for the hydraulic components.

3.2 | Additional Experimental Investigation

This section presents the results of a supplemental experimental analysis conducted to quantify the contribution of each noise source, both direct and indirect. In all reported comparisons, positive attenuations are to be interpreted as a reduction in the noise level within the cabin, and thus, as an improvement in the perceived acoustic quality.

3.2.1 | Investigation on silent blocks

In a preliminary stage of the investigation on the silent blocks, the cabin was decoupled from the transmission and suspended using elastic tie rods, while the hydraulic circuit remained active. Fig. 6 presents the attenuations recorded by the microphones relative to the baseline configuration.

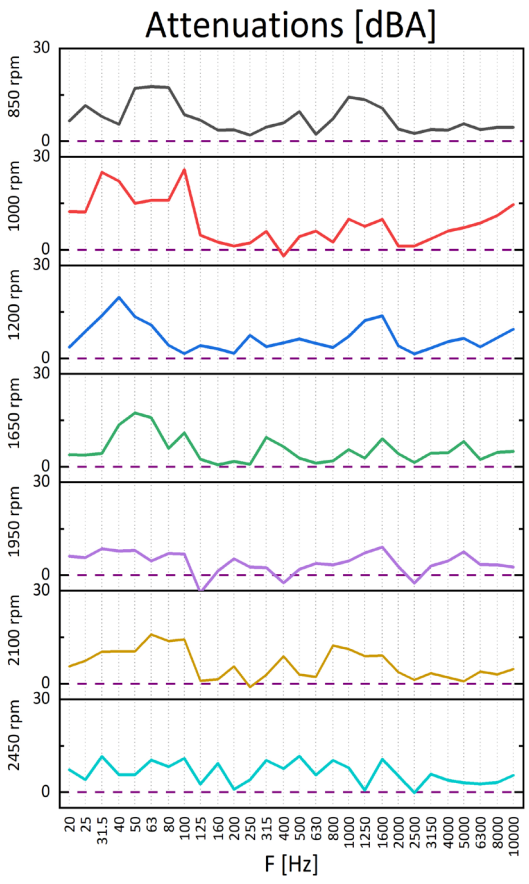

Fig. 6 – Acoustic attenuations in 1/3 octave bands following cabin suspension

Attenuazione in 1/3 di ottava ai microfoni a seguito della sospensione della cabina

The comparison shows that the cabin suspension exerts a significant effect at low frequencies, proving to be particularly effective in filtering the components associated with combus-

tion orders. Their efficiency tends to decrease between 125 Hz and 1000 Hz, an interval where hydraulic components persist, as previously highlighted, due to the maintenance of the hydraulic circuit. The decoupling continues to produce positive effects even in the frequency band between 1000 Hz and 2000 Hz.

The overall attenuations, illustrated in Fig. 7 for different rotation speeds, demonstrate a significant improvement in cabin noise for all rpm values, except at 1950 rpm, where a reduction of approximately 2 dBA is still measured. Negative attenuations are attributed to unintended mechanical contacts between the hydraulic lines and the cabin's structural elements, which introduce additional vibration components (mainly at the characteristic frequencies of the hydraulic sources) into the measured response.

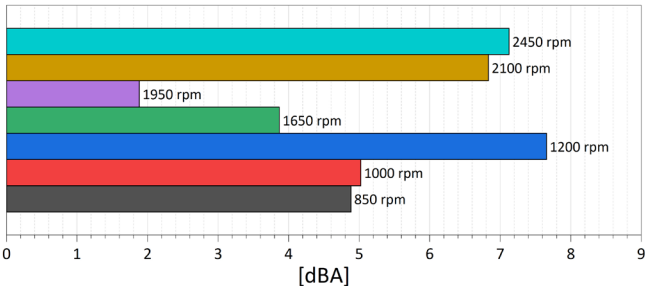

Fig. 7 – Acoustic attenuations following cabin suspension. Positive values indicate a reduction in internal noise

Attenuazioni globali ai microfoni a seguito della sospensione della cabina. Valori positivi indicano una riduzione della rumorosità interna

Following the results obtained with the suspension of the cabin, experimental tests were conducted by replacing the silent blocks of the baseline configuration with the following configurations:

- Type CB 80 silent blocks [15] maintaining the same geometry as the baseline configuration but with a hardness of 55 Shore (with a maximum load of 140 kg, utilized only in static conditions.
- Type CB 110 [16] silent blocks with modified geometry (diameter 100mm and thickness 105mm without any torque) and a hardness of 45 Shore.

Fig. 8 displays the attenuation ramps as a function of engine speed for the tests conducted with the 55 Shore and 45 Shore supports. From these comparisons, an average attenuation of approximately 1 dBA is observed for the supports 55 Shore, while the supports 45 Shore yield an average attenuation of around 3 dBA.

The performance of the silent blocks was also evaluated in the frequency domain, as illustrated in Fig. 9, which summarizes the attenuations relative to the baseline configuration at various frequencies. The curves were obtained by energetically averaging the spectra calculated from the ramps over a 1-second time interval.

The graphs indicate that both configurations exhibit attenuations at low frequencies, while showing critical behaviour (particularly for the stiffer supports) in the range between 160 Hz and 800 Hz, confirming the results obtained with the suspension of the cabin. Overall, it can be concluded that the 45 Shore silent blocks are significantly more effective than those tested, particularly in the frequency range between 1000 Hz and 2000 Hz.

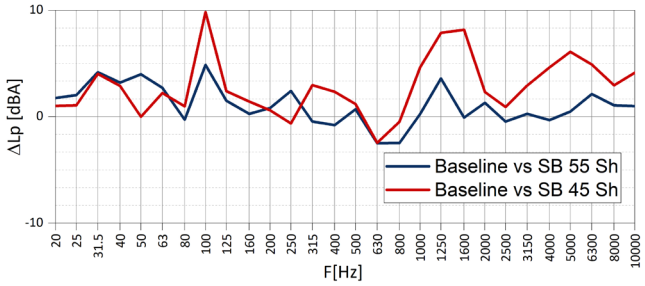

Fig. 9 – Noise attenuation in 1/3-octave bands compared to the baseline configuration as a function of engine RPM (a) Silent Blocks 55 Shore (b) Silent Blocks 45 Shore

Attenuazione ai microfoni in 1/3 di ottava rispetto alla configurazione base al variare del numero di giri (a) Supporti 55 Shore (b) Supporti 45 Shore

Fig. 10 compares the transmissibility functions between the silent blocks of the baseline configuration and those rated at 45 Shore. The increased filtering capacity is evident across nearly all frequencies of interest. The average increase in transmissibility ranges from 3 to 4 dB, which is consistent with the observed reduction in noise levels within the cabin.

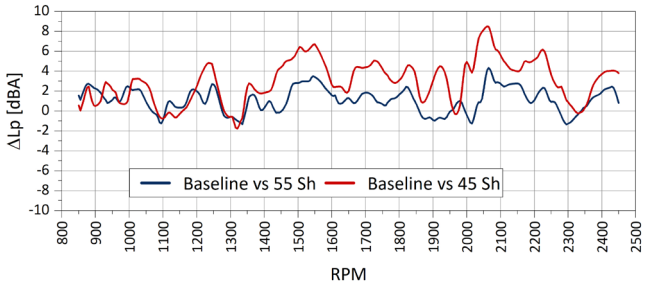

Fig. 8 – Overall noise attenuation as a function of engine RPM with alternative silent blocks compared to the baseline configuration

Attenuazione globale ai microfoni al variare dei giri motore con supporti antivibranti alternativi rispetto alla configurazione base

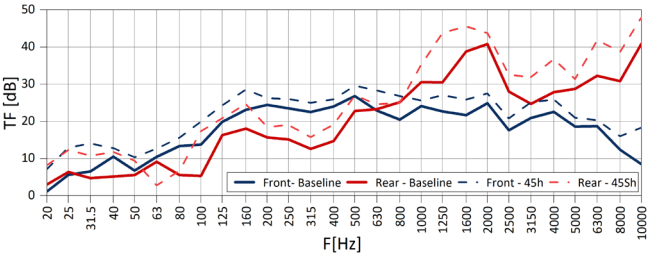

Fig. 10 – Transmissibility functions (in 1/3 octave bands): comparison between baseline and Silent Blocks 45 Shore

Funzioni di trasmissibilità (in 1/3 di ottava): confronto tra condizione base e supporti 45 Shore

3.2.2 | *Investigation on Propagation Paths*

The results presented in section 3.1 indicated that part of the noise contribution within the cabin originates from the vibrations of the firewall and the brake pipe connected to the front part of the cabin itself.

To evaluate the contribution of these elements, experimental tests were conducted in two different configurations. The first involved covering the firewall with a multi-layer insulating system composed of 10 mm PIR-PET material and 3.5 mm EPDM layer. The second configuration included replacing a section of the brake pipe with a flexible hose. These two configurations are illustrated in Fig. 11. It is important to note that these modifications maintain the original installation of the HSU and the brake pump on the firewall.

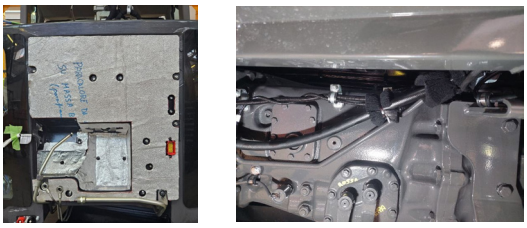

Fig. 11 – Modifications to propagation paths: (a) firewall coating (b) pipe decoupling

Interventi sui percorsi di propagazione: (a) rivestimento parafiamma (b) disaccoppiamento tubo

Fig. 12a presents the attenuation ramps as a function of engine speed for the microphones during the tests conducted in the two configurations earlier described. From these comparisons, an average attenuation of approximately 2.5 dBA is observed.

The performance of the two configurations was also evaluated in the frequency domain (Fig. 12b), where the attenuations are compared to the baseline configuration across various frequencies. The figure indicates that both configurations exhibit significant attenuations throughout the frequency spectrum of interest. Overall, a more distributed attenuation is observed, attributed to the decoupling of the pipes.

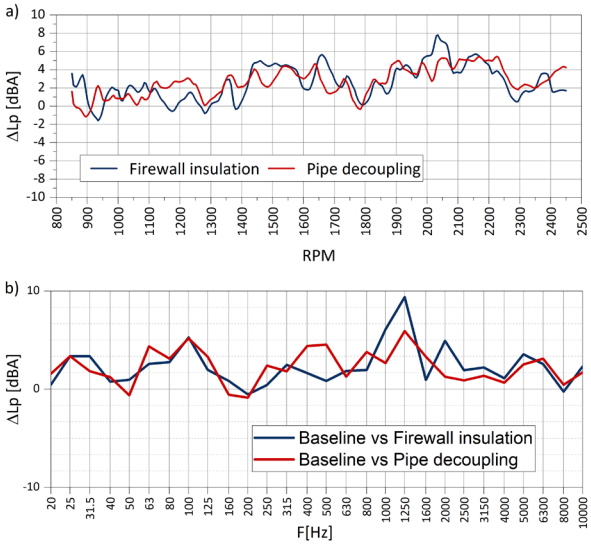

Fig. 12 – Attenuations following modifications to propagation paths: (a) overall values (b) 1/3-octave spectrum

Attenuazioni a seguito degli interventi sui percorsi di propagazione: (a) valori globali (b) spettro in 1/3 di ottava

3.2.3 | *Investigation on Sources*

The final phase of the investigation into primary noise sources involved extensive characterization in the following configurations:

- **HSU bypass**: the steering valve has been by-passed through a direct hydraulic connection of the inlet to the discharge port, keeping the valve in place at the steering column. In this way it has been determined the contribution of the steering unit to the noise transferred to the driver;
- **HSU and Brake Pump bypass**: in addition to the HSU bypass, the oil supply to the brake pump is interrupted by removing the feeding hose. By doing so, all the excitation sources to the cabin that are directly connected to the hydraulic circuit have been removed;
- **External Pump bypass**: the external pump has been removed in order to eliminate a source of excitation and determine the contribution of the displacement unit to the noise transferred to the cabin;
- **Dedicated pump for HSU**: a dedicated circuit is created for the power steering instead of connecting it in series with other oil consumers;
- **Silencer**: a multiple Helmholtz resonator aimed at reducing the amplitude of the pressure pulsation emitted by the displacement unit (Fig. 13). It is made of two concentric pipes: the inner one is the main oil duct where the oil flow takes place, the outer one defines the expansion chamber. Multiple holes drilled on the inner pipe allows the hydraulic connection between the volumes and define the number of necks of the frequency response. Also, the transmission loss of the device is properly calibrated by acting on resonance volume and bore shape. In particular, transmission loss peaks are shifted at lower frequency as the volume increase and by reducing the length to diameter ratio of the bores [17];
- **Silent Pump**: silenced fixed displacement unit (Fig. 14). The gear wheels have seven teeth that combine helical gearing with a non-involute tooth profile allowing a permanent tooth contact. Moreover, the peculiar gearing shape prevents local pressure peaks between the tooth

Fig. 13 – Silencer

Silenziatore

Fig. 14 – Silent pump
Pompa silenziata

flanks, that is one of the main disadvantages of spur gears pumps on the noise and vibration point of view. Such characteristics result in a strongly reduced flow pulsation compared to standard external gear pumps.

The microphone attenuations at various engine speeds are presented in Fig. 15. From these comparisons, it is observed that all configurations (except for the external bypass pump) have a significant effect at low speeds (850 rpm). Among the tested configurations, the HSU bypass, the HSU and brake pump bypass, and the dedicated pump for HSU show negligible effects above 1000 rpm. The remaining configurations lead to a significant reduction in noise, with the silent pump providing the best overall performance.

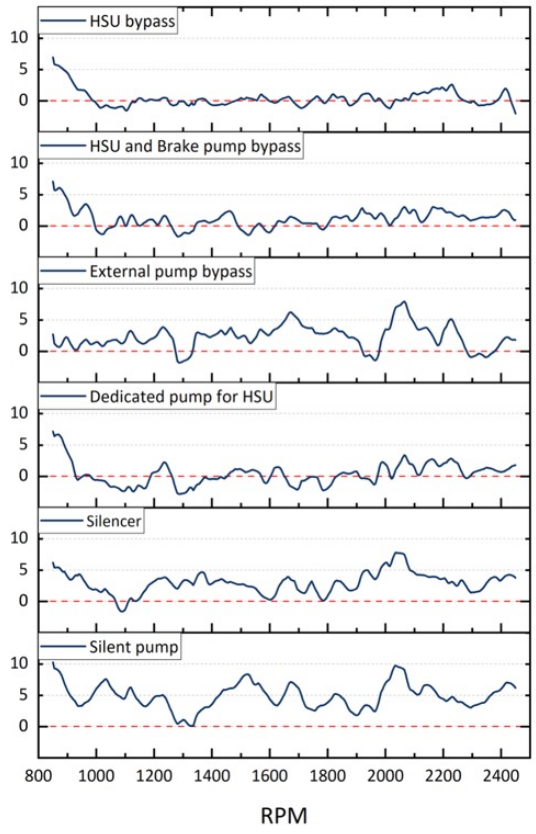

Fig. 15 – Overall noise attenuation as a function of engine RPM, for all modifications to the main sources compared to the baseline configuration
Attenuazione globale ai microfoni al variare dei giri motore per tutti gli interventi sulle sorgenti principali rispetto alla configurazione base

The global attenuations for the various rpm values shown in Fig. 16 indicate a significant improvement at all rpm levels, except at 1650 rpm, where the attenuation is approximately 2 dBA.

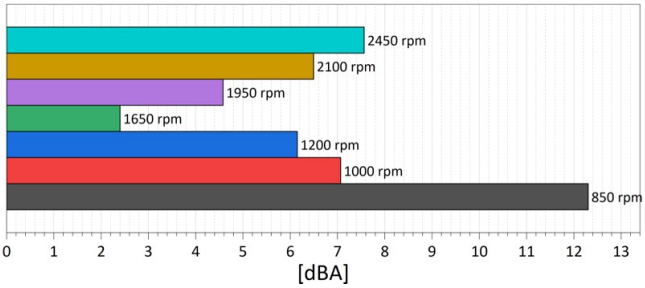

Fig. 16 – Overall acoustic attenuations with silent pump
Attenuazioni globali ai microfoni nella condizione di pompa silenziata

3.2.4 | Results resume

In the following section, the results of the additional experimental campaign are summarized by dividing the entire frequency range into three segments:

- **Range 1**: Energy content between 20 Hz and 125 Hz. In this range, contributions primarily related to the combustion mechanism are observed, along with potential anomalies linked to gear interactions in unfavourable cases.
- **Range 2**: Energy content between 160 Hz and 800 Hz. In this range, the major contribution comes from the hydraulic circuit (fundamental harmonic and its first harmonics).
- **Range 3**: Energy content above 1000 Hz. This range has a significant impact in terms of mechanical noise, predominantly arising through the silent blocks and the firewall.

Starting from the frequency spectra obtained for each of the analysed configurations, global values (as the energetic sum of frequency components) were determined for the three representative ranges. The attenuations relative to the baseline configuration are shown in figures 17(a)-(c). Fig. 15(d) presents the microphone attenuations averaged over all engine speed values.

The data summarized in Fig. 17 indicate that, excluding the suspension of the cabin, the interventions with the most significant effect on noise reduction are primarily the use of the silent pump and the 45 Shore silent blocks. Additionally, for Range 2, the decoupling of the pipes also contributes notably. The silencer has a non-negligible effect (particularly in Range 2), but it is still less effective than the silent pump. The effects of the bypasses for the pumps and the HSU can be considered relatively insignificant.

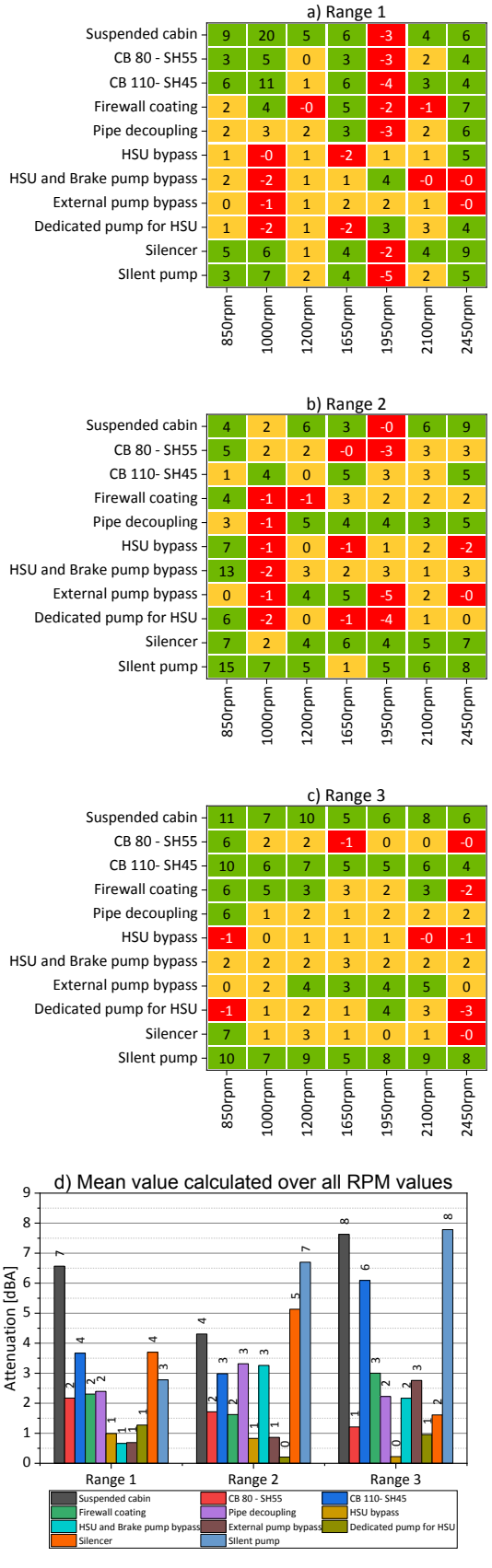

Fig. 17 – Overall noise attenuation as a function of engine RPM, for all modifications to the main sources compared to the baseline configuration (a) Range 1 (b) Range 2 (c) Range 3 (d) Average for all RPM values

Attenuazione globale ai microfoni al variare dei giri motore per tutti gli interventi sulle sorgenti principali rispetto alla configurazione base(a) Range 1 (b) Range 2 (c) Range 3 (d) Media su tutti i valori di rpm

3.3 | Optimized configuration

3.3.1 | *Experimental results*

Based on the synthesis presented in the previous section, the final phase of the activity involved repeating the tests using an optimized configuration consisting of a silent pump, 45 Shore silent blocks, and the decoupling of the brake pipe. The main results are presented in Figs. 18 and 19.

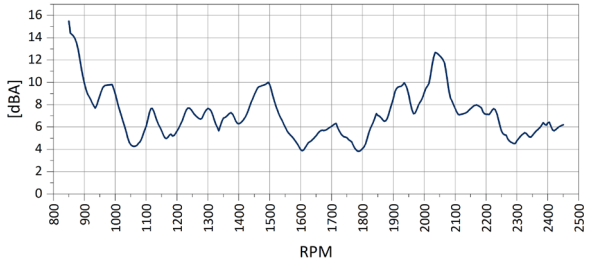

Fig. 18 – Overall noise attenuation as a function of engine RPM, for the optimized configuration compared to the baseline

Attenuazione globale ai microfoni al variare dei giri motore per la configurazione ottimizzata rispetto alla configurazione di base

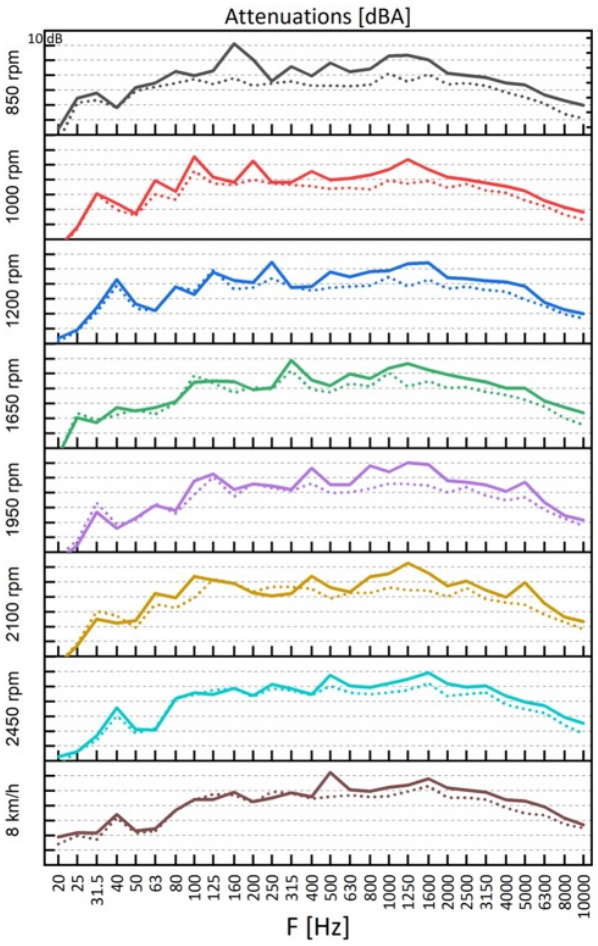

Fig. 19 – Frequency spectra of the microphone envelope for the baseline configuration (solid line) and the optimized configuration (dashed line) as a function of the rotational speed

Spettri in frequenza dell'inviluppo dei microfoni per le configurazioni base (linea continua) e ottimizzata (linea tratteggiata) al variare del numero di giri

In particular, the ramp of overall sound pressure envelope as a function of engine speed shows a significant attenuation averaging approximately 7 dBA, with values around 14 dBA at idle. In spectral terms, the optimized configuration is able to significantly reduce the hydraulic components and noise at frequencies above 1000 Hz.

Finally, Fig. 20 presents the spectrogram of the envelope from the microphones during a static measurement for the optimized configuration.

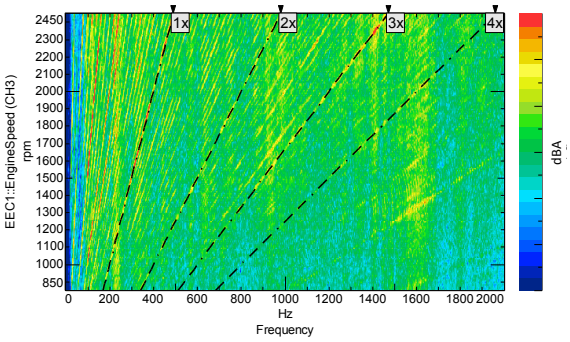

Fig. 20 – Spectrogram of sound pressure levels a static measurement varying the rotational speed for the optimized configuration

Spettrogramma del livello sonoro per una misura statica variando in rampa continua il numero di giri per la configurazione ottimizzata

The spectrogram, when compared with the equivalent graph shown in Figure 1 for the baseline, clearly illustrates the improvement in noise levels as the rotational speed varies and across all frequencies of interest.

3.3.2 | Definition of a ML-based predictive model of Internal Noise

This section will define a predictive model for the overall internal noise (in dBA) based on the global acceleration values (in dB ref. 1g) at various positions of the accelerometric sensors.

Figure 21 summarizes the primary effects of each tested configuration on the accelerometer locations. As an example, configurations involving different silent blocks mainly affect the cabin upstream and downstream sensors and the handbrake, as expected from their mechanical coupling paths. In contrast, the configurations using the silencer and the silent pump produce responses across all accelerometers, indicating a more global influence on the vibration field.

Subsequently, the correlations between the trends of the global values at the microphones and the global values at each individual accelerometer were calculated (Fig. 22). The quality of the correlation was assessed using the linear correlation coefficient.

While the analysis of individual linear correlation coefficients identifies the points with the most significant effects, in a complex system such as the one analysed, it is reasonable to assume that noise levels may be associated with a combination of one or more variables.

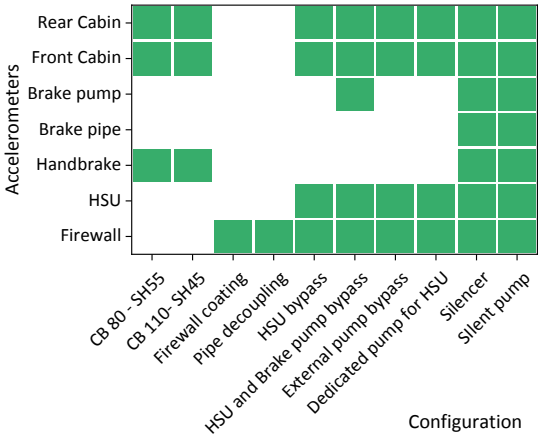

Fig. 21 – Effect of the tested configurations at the various accelerometer positions

Effetto delle configurazioni testate alle varie posizioni accelerometriche

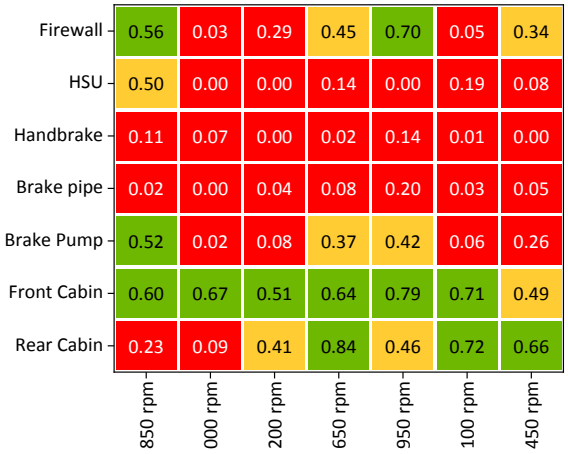

Fig. 22 – Linear correlation coefficients between noise and vibration sensors

Effetto delle configurazioni testate alle varie posizioni accelerometriche

Using a machine learning approach [18-20] a predictive model was developed based on a multivariate polynomial of the form:

$$M = \alpha_0 + \sum_{j=1}^{7}\sum_{k=1}^{n} \alpha_{jk} x_j^k + \sum_{j<1}\sum_{a+b<n} \beta_{j,a,b} x_j^a x_j^b \qquad (1)$$

where:

- x_j are the variables (firewall, HSU, handbrake, etc.);
- α_j are the coefficients of the individual powers;
- $\beta_{j,a,b}$ are the coefficients of the interactions up to the degree n.

From a preliminary study, a polynomial degree of $n = 4$ ensures the convergence of the result. The validation of the model was conducted by attempting to predict the internal noise of the optimized configuration after assigning a new set of variables related to that configuration. The differences between the measured and estimated noise values are presented in Fig. 23.

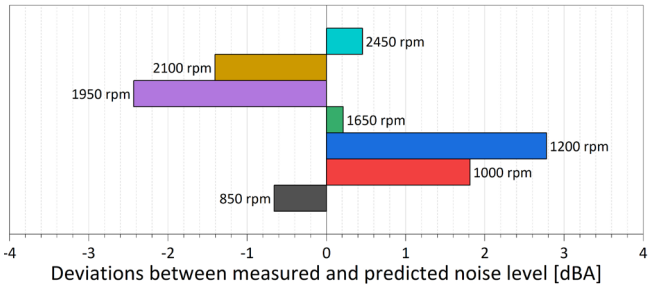

Fig. 23 – Difference between the measured noise and the noise estimated by the predictive model for the optimized configuration

Differenza tra rumorosità misurata e stimata mediante il modello predittivo per la configurazione ottimizzata

4 | Conclusions

The work conducted enabled a comprehensive experimental analysis of an agricultural tractor, with the primary objective of reducing perceived noise within the operator cabin. Measurements of sound pressure levels inside the cabin, combined with accelerometric data collected at several critical points on the machine, provided an initial characterization of vibration sources and propagation paths. This preliminary phase was essential for identifying dominant contributors to cabin noise and establishing correlations between structural dynamics and acoustic response.

Building on these findings, targeted interventions were implemented to isolate and mitigate the main noise sources. These actions included modifications to propagation paths, the integration of anti-vibration mounts (silent blocks), and adjustments to specific components acting as primary sources of excitation. The most effective measures were combined to define an optimized configuration capable of significantly reducing cabin sound levels across the entire engine speed range. Comparative analyses confirmed that this configuration achieved substantial improvements in acoustic comfort without compromising operational performance.

Furthermore, leveraging the observed correlations between accelerometric signals and microphone measurements, a preliminary predictive model was developed. This model, experimentally validated on the optimized configuration, demonstrated an accuracy of approximately 3 dBA in estimating cabin noise levels. Such predictive capability represents a valuable tool for early-stage design optimization, reducing reliance on extensive physical testing.

Future developments will focus on extending the applicability of the predictive model by increasing sensor density and incorporating additional parameters. These enhancements aim to improve model robustness and enable its integration into advanced NVH simulation frameworks, supporting the design of next-generation agricultural tractors with superior acoustic performance.

Conclusioni

L'attività presentata nell'articolo ha permesso di effettuare un'analisi sperimentale completa su un trattore agricolo, con l'obiettivo principale di ridurre il rumore percepito all'interno della cabina operatore. Le misurazioni dei livelli di pressione sonora all'interno della cabina, combinate con i dati accelerometrici raccolti in diversi punti critici della macchina, hanno fornito una caratterizzazione preliminare delle sorgenti di vibrazione e dei percorsi di propagazione. Questa fase iniziale è stata fondamentale per identificare i principali contributi al rumore in cabina e stabilire correlazioni tra la dinamica strutturale e la risposta acustica.

Sulla base di tali risultati, sono stati implementati interventi mirati per isolare e mitigare le principali sorgenti di rumore. Le azioni hanno incluso modifiche ai percorsi di propagazione, l'integrazione di supporti antivibranti (silent block) e l'ottimizzazione di componenti specifici responsabili delle eccitazioni principali. Le misure più efficaci sono state combinate per definire una configurazione ottimizzata, capace di ridurre in modo significativo i livelli sonori in cabina lungo l'intero intervallo di velocità del motore. Le analisi comparative hanno confermato che tale configurazione ha ottenuto miglioramenti sostanziali in termini di comfort acustico senza compromettere le prestazioni operative.

Inoltre, sfruttando le correlazioni osservate tra i segnali accelerometrici e le misurazioni microfoniche, è stato sviluppato un modello predittivo preliminare. Questo modello, validato sperimentalmente sulla configurazione ottimizzata, ha dimostrato un'accuratezza di circa 3 dBA nella stima dei livelli di rumore in cabina. Tale capacità predittiva rappresenta uno strumento prezioso per l'ottimizzazione progettuale nelle fasi iniziali, riducendo la dipendenza da test fisici estensivi.

Gli sviluppi futuri si concentreranno sull'estensione dell'applicabilità del modello predittivo mediante l'aumento della densità dei sensori e l'inclusione di ulteriori parametri significativi. Questi miglioramenti mirano a incrementare la robustezza del modello e consentirne l'integrazione in avanzati framework di simulazione NVH, supportando la progettazione di trattori agricoli di nuova generazione con prestazioni acustiche superiori.

References

[1] A. Pretzsch, A. Seidler, J. Hegewald, Health Effects of Occupational Noise. Curr Pollution Rep 7, 344–358 (2021). https://doi.org/10.1007/s40726-021-00194-4.

[2] L.K. Kanu, S.M.K. Lwara, X. Meng, Impacts of workplace noise exposure and mitigation strategies: a scoping review. Discov Public Health 22, 214 (2025). https://doi.org/10.1186/s12982-025-00611-9.

[3] Directive 2003/10/EC – noise (latest update: 14/11/2024), https://osha.europa.eu/en/legislation/directives/82 (accessed November 20, 2025).

[4] Regulation (EU) 1322/2014, https://eur-lex.europa.eu/eli/reg_del/2014/1322/oj/ita (accessed November 20, 2025).

[5] Regulation (EU) 167/2013 https://eur-lex.europa.eu/eli/reg/2013/167/oj/eng (accessed November 20, 2025).

[6] T.K. Mahapatra, S. Satapathy, (2024). Assessment and Evaluation of the Effects of Hazardous Noise Produced by the Manufacturing Industry on the Workers. In: Realyvásquez Vargas, A., Satapathy, S., García Alcaraz, J.L. (eds) Automation and Innovation with Computational Techniques for Futuristic Smart, Safe and Sustainable Manufacturing Processes. Springer, Cham. https://doi.org/10.1007/978-3-031-46708-0_6.

[7] E. Carletti, G. Miccoli. Vibroacoustic Optimization of a Tractor Cab. 21st International Congress on Sound and Vibration, Beijing. 2014.

[8] M. Martelli, D. Chiarabelli, S. Gessi, P. Marani, E. Mucchi, M. Polastri, Comprehensive lumped parameter and multibody approach for the dynamic simulation of agricultural tractors with tyre-soil interaction. IET Cyber-Syst. Robot. e12092, 2023. https://doi.org/10.1049/csy2.12092.

[9] G. Pasch, G. Jacobs, J. Berroth. NVH System Simulation of a Tractor with Hydrostatic-Mechanical Power Split Transmission. Landtechnik, 75(4):301–315. DOI: 10.15150/lt.2020.3254. 2020.

[10] F. Mori, A. Santoni, P. Fausti, F. Pompoli, P. Nataletti, P. Bonfiglio. The effectiveness of an active noise control system with remote microphones technique in a tractor cabin. Rivista Italiana di Acustica. DOI: 10.3280/ria1-2025oa19189. 2025.

[11] M.-W. Kang, H.-W. Han, Y.-J. Park. Optimization of Cabin Mounting System for Tractor using a Genetic Algorithm. Journal of Biosystems Engineering. DOI: 10.1007/s42853-024-00217-0. 2024.

[12] P. Cardei, C. Sorica, V. Vladut, M. Matache. Studies on the Experimental Validation of the Theoretical Static Noise Field in the Neighbourhood of Agricultural Tractors. Springer Proceedings in Physics. DOI: 10.1007/978-3-030-54136-1_17. 2020.

[13] F. Pedrielli, E. Carletti, P. Fausti, F. Pompoli, A. Peretti, J. Griguolo, P. Nataletti. Analysis of the psychoacoustic parameters in agricultural tractor cabs. Conference Proceedings. 2018.

[14] A. Peretti, J. Griguolo, F. Pompoli, C. Visentin, P. Fausti, F. Pedrielli, E. Carletti, P. Nataletti. Misure su trattori agricoli finalizzate all'individuazione delle caratteristiche delle vibrazioni e del rumore nonché delle dotazioni e configurazioni più adeguate. AIA Conference. 2018.

[15] AMC-MECANOCAUCHO® type CB80 www.mecanocaucho.com/en/products/anti-vibration-mount/cb/#plano-5 (accessed November 20, 2025).

[16] AMC-MECANOCAUCHO® type CB110 www.mecanocaucho.com/en/products/anti-vibration-mount/cb/#plano-6 (accessed November 20, 2025).

[17] M. Kohlberg, F. Thielecke, U. Heise, R.M. Behr, Novel concepts for noise reduction in aircraft hydraulic systems, Deutscher Luft- und Raumfahrtkongress (DLRK), Bremen, Germany, September 27-29, 2011.

[18] D.C. Montgomery, E. A.Peck, G.G. Vining, Introduction to Linear Regression Analysis, 6th edition. Wiley, 2021.

[19] T. Hastie, R.Tibshirani, J. Friedman. The Elements of Statistical Learning: Data Mining, Inference, and Prediction, Springer, 2009.

[20] G.A.F. Seber, A.J. Lee, Linear Regression Analysis, 2nd edition, Wiley, 2003.